Reduced chemistry and differential diffusion effects in simulations of ammonia-hydrogen fuel blend

Giovanni Grassi, Pascale Domingo, Luc Vervisch
CORIA-CNRS, Normandie Université, INSA de Rouen Normandie
Saint-Etienne-du-Rouvray, France

1 Introduction

Ammonia is increasingly recognized worldwide as a promising carrier for hydrogen and energy. One effective strategy is blending ammonia with hydrogen to achieve combustion characteristics comparable to those of natural gas, including stable flame anchoring, controlled flame length, and sufficient heat release for energy production. The design and optimization of ammonia combustion systems rely heavily on computational fluid dynamics (CFD). Accurate CFD simulations require chemical kinetic models that strike a balance between simplicity and fidelity, minimizing computational complexity while effectively capturing the essential thermochemistry of hydrogen-enriched ammonia combustion. This study begins with a detailed ammonia/air combustion mechanism and examines the impact of a canonical problem on chemical mechanism reduction. The methodology employs automated analyses to identify the most influential chemical species and elementary reactions. Three key reactive scenarios are explored: ignition with and without micro-mixing, freely propagating laminar premixed flames, and strained counterflow diffusion flames near quenching conditions. This comprehensive approach facilitates the development of reduced kinetic models specifically tailored to ammonia/hydrogen-air combustion under various operating conditions. Subsequently, the reduced chemical schemes are utilized to conduct direct numerical simulations of ammonia-hydrogen-air mixing layers. The impact of differential diffusion on the definition of the mixture fraction is examined, in the context of its potential role as an input parameter for detailed chemistry tabulation.

2 Canonical problems and chemistry reduction

The detailed chemical model used is C3MECHV3.5, developed by merging various high-fidelity mechanisms, with NUIGMech1.1 as the core and NO_x chemistry from NUI Galway [1]. Additional submechanisms are outlined by Dong et al [2]. The initial version, C3MECHV3.3, was then updated and experimentally validated for ammonia combustion over a wide range of conditions.

The ORCh package is used to reduce the chemistry [3, 4]. The generation of reduced/optimized models is based on the coupling of two different procedures, the reduction of the number of reactions and species using Directed Relation Graph with error propagation (DRGEP) [5, 6] and the optimization of the reaction rate constants using Genetic Algorithm [3, 7]. The reduction and optimization processes

Correspondence to: giovanni.grassi@insa-rouen.fr

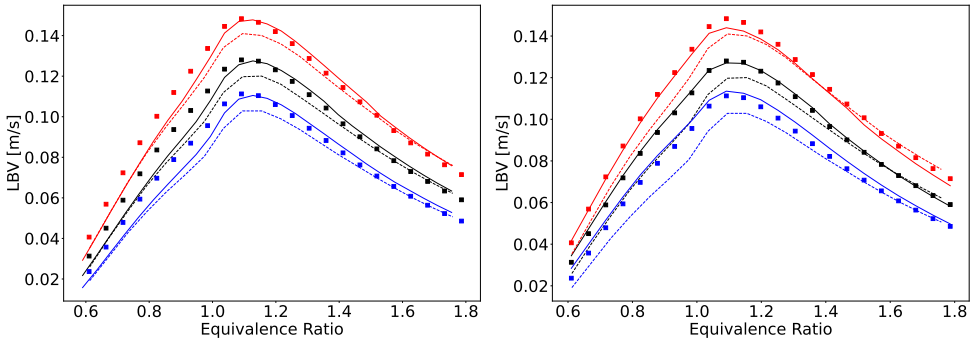

(a) RmAH-1 (b) RmAH-2

Figure 1: Laminar burning velocity vs equivalence ratio. Blue: Hydrogen fraction of 10 % by volume; black: 15 %; red: 20 % . Symbol: Detailed scheme [2]. Dashed line: reduced (no optimization). Solid line: reduced + optimized, (a): RmAH-1, (b): RmAH-2 (Table 1).

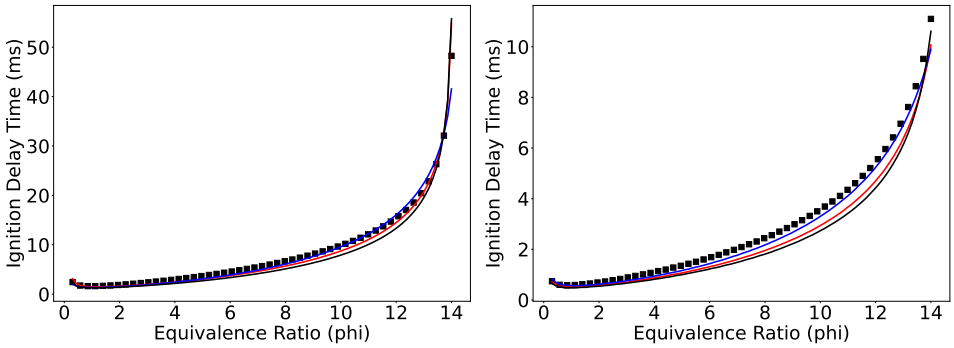

(a) $X_{H_2} = 10\%$ (b) $X_{H_2} = 20\%$

Figure 2: Ignition delay time (ms) vs equivalence ratio. Symbol: Detailed scheme [2]. Red: RmAH-1, blue: RmAH-2 (Table 1), black: no-optimization.

are conducted using canonical problems: 0D ignition with non-premixed stochastic micro-mixing and one-dimensional freely propagating premixed flames. The 0D ignition problem with stochastic mixing encompasses the full range of operating conditions in the composition-temperature space, simulating scenarios with three injection zones comprising fuel, air, and burnt gases. This setup mimics a boiler environment where recirculated burnt gases dilute the reactants, aiding in both ignition and flame stabilization. One-dimensional freely propagating flames are computed at different equivalence ratios of the fuel/air mixture, and both species profiles through the flame and laminar burning velocity are studied to ensure accurate predictions of the Laminar Burning Velocity (LBV). Other flame properties, such as the diffusion flame quenching point under a small Damkohler number, are also examined. However, these simulations of counterflow diffusion flames are only used for testing and are not involved in the reduction process. By employing two optimization sequences tailored to the canonical problems (A: 0D+premixed+OD+premixed; B: 0D+premixed), two slightly different reduced schemes, RmAH-1 and RmAH-2, consisting of 19 species and 75 reactions, have been developed (Table 1).

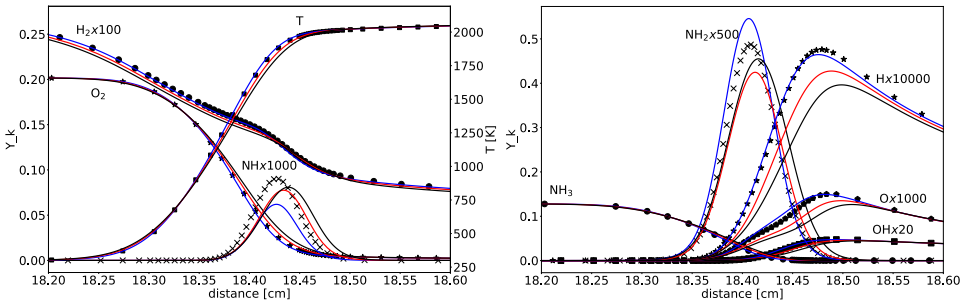

(a) T, H_2, O_2, NH (b) NH_3, NH_2, H, O, OH

Figure 3: Stoichiometric premixed flame, 15% H_2 in fuel. Temperature and species mass fractions. Symbol: Detailed scheme [2]. Red: RmAH-1, blue: RmAH-2 (Table 1), black: no-optimization.

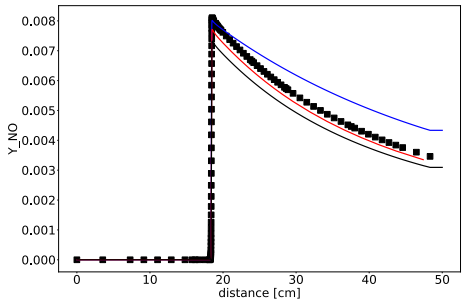

Figure 4: Stoichiometric premixed flame, 15% H_2 in fuel. NO mass fraction. Symbol: Detailed scheme [2]. Red: RmAH-1, blue: RmAH-2 (Table 1), black: no-optimization.

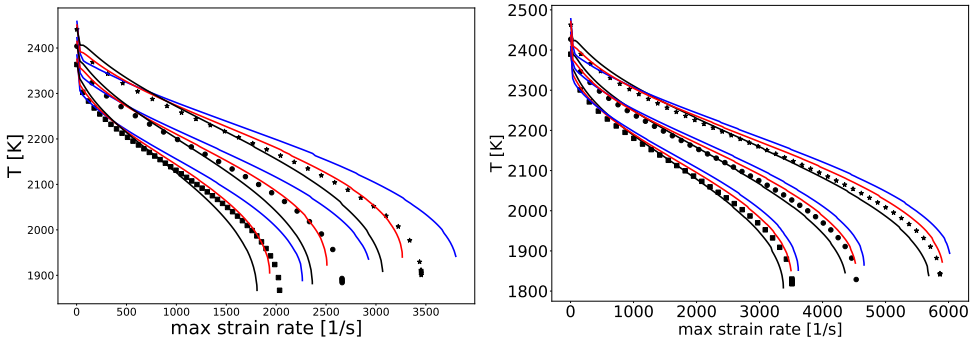

(a) 10% H_2 (b) 15% H_2

Figure 5: Maximum temperature vs maximum strain rate s^{-1} in an opposed-jet diffusion flame. Symbols detailed scheme [2], square: preheated air at 800K, circle: 900K, star: 100K. Red: RmAH-1, blue: RmAH-2 (Table 1), black: no-optimization.

3 Analysis of the reduced schemes

RmAH-1 demonstrates higher accuracy in predicting most species responses, including the maximum burning velocity of the premixed flame (Fig. 1(a)). Conversely, RmAH-2, being more specifically constrained to reproduce premixed flames, achieves greater accuracy on the lean side (Fig. 1(b)), while ignition delay without micro-mixing are better reproduced with RmAH-2 (Fig. 2). Looking at the species distribution in premixed flames (Fig. 3), both schemes performs quite well. However, RmAH-1 demon-

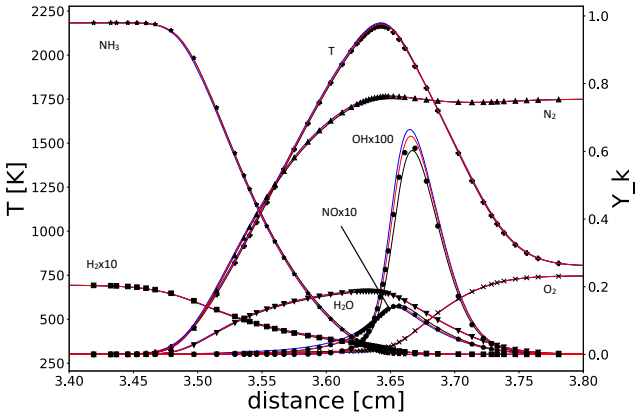

Figure 6: Strained (400 s^{-1}) diffusion flame. Temperature and species mass fractions. Symbol: Detailed scheme [2]. Red: RmAH-1, blue: RmAH-2 (Table 1), black: no-optimization.

strates superior precision in capturing the NOx pathway, particularly the slow DeNOx process observed in the burnt gases (Fig. 4).

In a counterflow diffusion-strained flame simulation conducted with Cantera [8], the oxidizer stream temperature was varied to assess the performance of both schemes in predicting flame quenching. The results, presented in Fig. 5, reveal that RmAH-1 outperforms RmAH-2 in accurately predicting the quenching point, with both schemes capturing the chemical structure of the reaction zone (Fig. 6). As anticipated, the reduced scheme not optimized using the genetic algorithm exhibits significant deviations in predicting the quenching strain rate under all tested conditions (Fig. 5).

These results highlight the importance of chemical mechanism reduction under the specific operating conditions targeted for subsequent use in CFD simulations.

5 Mixing layer and multi-fuel mixture fraction

A two-dimensional mixing layer is simulated with the detailed and reduced schemes using the reactive flow solver SiTCom-B (www.coria-cfd.fr/index.php/SiTCom-B). The upper stream consists of preheated air at 1700 K with a mean velocity of 39.6 $m{\cdot}s^{-1}$ and a cold wall maintained at 600 K. Below an adiabatic splitter plate, the lower stream comprises a mixture of ammonia and hydrogen (15% by volume) at ambient temperature (300 K) with a velocity of 15 $m{\cdot}s^{-1}$. Additionally, 10% velocity fluctuations are introduced as homogeneous turbulence. Figure 7 illustrates that, accounting for flow and molecular transport, both reduced schemes effectively capture the flame dynamics and NO production.

The definition of the mixture fraction in cases involving fuel blends and differential diffusion is not universally established [10]. Figure 8 illustrates significant variations in the stoichiometric mixture fraction's position within the flow, depending on whether it is defined solely based on atomic elements (e.g., H, N, and O) or using Bilger's formulation [9]. This departure results from differential diffusion. The stoichiometric line of the mixture fraction solely based on the H atom appears as the best tracer of the maximum of heat release heat surface. Bilger's formulation also appears to be quite effective. Single-step chemistry-based mixture fraction ($\nu_{\mathrm{NH_3}}\mathrm{NH_3} + \nu_{\mathrm{H_2}}\mathrm{H_2} + \nu_{\mathrm{O_2}}\mathrm{O_2} \rightarrow \mathrm{Products}$),

$$Z = \frac{\phi_{\mathrm{NH_3}}(Y_{\mathrm{NH_3}}/Y_{\mathrm{NH_3},1}) + \phi_{\mathrm{H_2}}(Y_{\mathrm{H_2}}/Y_{\mathrm{H_2},1}) - (Y_{\mathrm{O_2}}/Y_{\mathrm{O_2},0}) + 1}{\phi_{\mathrm{NH_3}} + \phi_{\mathrm{H_2}} + 1}\,, \tag{1}$$

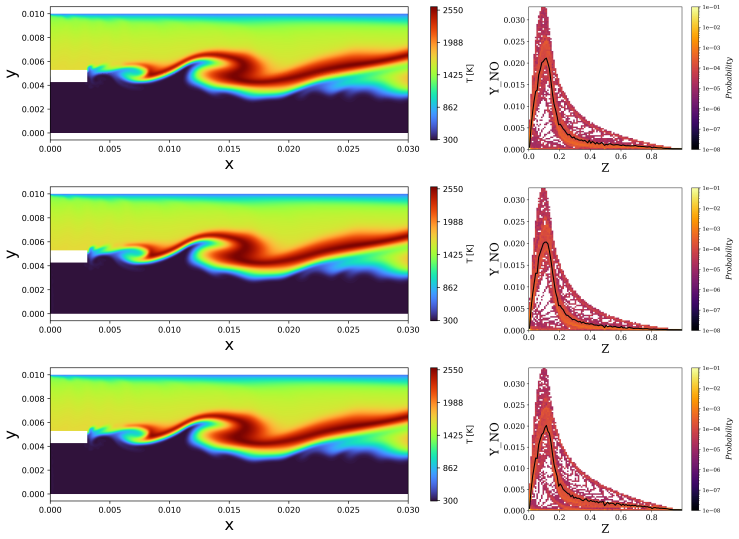

Figure 7: Mixing layer DNS. Top: detailed scheme. Middle: RmAH-1. Bottom: RmAH-2. Left: Temperature distribution. Right: scatter plots of NO concentration vs Bilger's mixture fraction [9]. Black: conditional mean. Green: stoichiometric iso-line

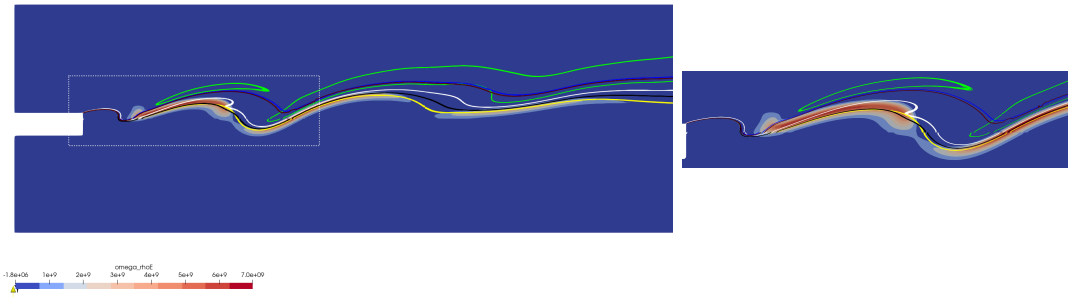

Figure 8: Heat release rate (J·m^{-3}) and stoichiometric mixture fractions. White: Z_{O}. Green: Z_{N}. Yellow: Z_{H}. Black: Z_{Bilger} [9]. Blue: Z_s and Brown Z_{L_s}. Right: zoom in the stabilization zone (white dashed box).

with $\phi_{\mathrm{NH_3}} = (\nu_{\mathrm{O_2}} Y_{\mathrm{NH_3},1})/(2\nu_{\mathrm{NH_3}} Y_{\mathrm{O_2},0})$ and $\phi_{\mathrm{H_2}} = (\nu_{\mathrm{O_2}} Y_{\mathrm{H_2},1})/(2\nu_{\mathrm{H_2}} Y_{\mathrm{O_2},0})$, or calibrated for non-unity Lewis number [11],

$$Z_L = \frac{\Phi_{\mathrm{NH_3}}(Y_{\mathrm{NH_3}}/Y_{\mathrm{NH_3},1}) + \Phi_{\mathrm{H_2}}(Y_{\mathrm{H_2}}/Y_{\mathrm{H_2},1}) - (Y_{\mathrm{O_2}}/Y_{\mathrm{O_2},0}) + 1}{\Phi_{\mathrm{NH_3}} + \Phi_{\mathrm{H_2}} + 1}\,, \tag{2}$$

with $\Phi_{\mathrm{NH_3}} = (Le_{\mathrm{O_2}}/Le_{\mathrm{NH_3}})\phi_{\mathrm{NH_3}}$ and $\Phi_{\mathrm{H_2}} = (Le_{\mathrm{O_2}}/Le_{\mathrm{H_2}})\phi_{\mathrm{H_2}}$ computed locally, feature stoichiometric values that poorly locates the maximum heat release rate. These commonly used definitions of the mixture fraction should be avoided when tabulating NH_3-H_2 complex chemistry. This is particularly true in the stabilization zone (see zoom in Fig. 8).

Table 1: Reactions and Arrhenius constants for both the mechanism: RmAH-1 and RmAH-2

n	Reaction Equation	RmAH-1			RmAH-2		
		A	b	E (J/mol)	A	b	E (J/mol)
1	$H_2 + O \rightleftharpoons H + OH$	$2.64e+09$	0.00	$3.27e+07$	$8.52e+09$	0.00	$3.30e+07$
2	$H_2 + O \rightleftharpoons H + OH$	$1.17e+12$	0.00	$8.09e+07$	$9.37e+11$	0.00	$8.30e+07$
3	$H_2 + OH \rightleftharpoons H + H_2O$	$2.15e+05$	1.52	$1.45e+07$	$1.50e+05$	1.53	$1.41e+07$
4	$H + O_2 \rightleftharpoons O + OH$	$1.04e+11$	0.00	$6.31e+07$	$1.26e+11$	0.00	$6.50e+07$
5	$H + OH + (^+M) \rightleftharpoons H_2O + (^+M)$	$3.28e+10$	0.23	$-4.64e+05$	$2.39e+10$	0.23	$-4.48e+05$
6	$2\,OH \rightleftharpoons H_2O + O$	$2.65e+03$	1.79	$-6.92e+06$	$2.71e+03$	1.76	$-7.00e+06$
7	$H + HO_2 \rightleftharpoons H_2 + O_2$	$2.69e+03$	2.08	$-5.75e+06$	$3.75e+03$	2.11	$-5.73e+06$
8	$H + HO_2 \rightleftharpoons 2\,OH$	$1.07e+11$	0.00	$1.24e+06$	$1.05e+11$	0.00	$1.24e+06$
9	$HO_2 + O \rightleftharpoons O_2 + OH$	$3.04e+10$	0.00	$0.00e+00$	$2.05e+10$	0.00	$0.00e+00$
10	$HO_2 + OH \rightleftharpoons H_2O + O_2$	$6.57e+16$	-2.47	$2.46e+06$	$1.87e+17$	-2.47	$2.46e+06$
11	$HO_2 + OH \rightleftharpoons H_2O + O_2$	$1.02e+06$	1.24	$-5.23e+06$	$1.54e+06$	1.25	$-5.20e+06$
12	$H + O_2 (^+M) \rightleftharpoons HO_2 (^+M)$	$3.48e+09$	0.44	$0.00e+00$	$3.41e+09$	0.43	$0.00e+00$
13	$NH_3 + M \rightleftharpoons H + NH_2 + M$	$3.90e+13$	0.00	$3.85e+08$	$1.01e+14$	0.00	$3.85e+08$
14	$H + NH_3 \rightleftharpoons H_2 + NH_2$	$2.38e+03$	2.24	$4.32e+07$	$1.90e+03$	2.25	$4.37e+07$
15	$NH_3 + O \rightleftharpoons NH_2 + OH$	$9.33e-02$	3.27	$1.53e+07$	$9.33e-02$	3.34	$1.51e+07$
16	$NH_3 + OH \rightleftharpoons H_2O + NH_2$	$1.00e+02$	2.37	$-7.11e+05$	$1.40e+02$	2.40	$-7.20e+05$
17	$NH_2 + M \rightleftharpoons H + NH + M$	$1.35e+12$	0.00	$3.21e+08$	$2.40e+11$	0.00	$3.18e+08$
18	$H + NH_2 \rightleftharpoons H_2 + NH$	$1.20e+03$	2.19	$6.80e+06$	$1.56e+03$	2.15	$7.02e+06$
19	$NH_2 + O \rightleftharpoons NH + OH$	$1.13e+10$	0.00	$0.00e+00$	$8.64e+09$	0.00	$0.00e+00$
20	$NH_2 + O \rightleftharpoons NH + OH$	$8.60e-04$	3.97	$6.99e+06$	$8.60e-04$	4.09	$6.83e+06$
21	$NH_2 + OH \rightleftharpoons H_2O + NH$	$3.87e+03$	1.95	$-8.58e+05$	$3.39e+03$	1.91	$-8.58e+05$
22	$2\,NH_2 \rightleftharpoons NH + NH_3$	$5.64e-03$	3.54	$2.31e+06$	$5.64e-03$	3.50	$2.30e+06$
23	$NH_2 + O \rightleftharpoons H + HNO$	$1.47e+12$	-0.50	$3.53e+06$	$1.22e+12$	-0.50	$3.43e+06$
24	$NH_2 + O \rightleftharpoons H + HNO$	$1.58e+11$	-0.24	$2.74e+06$	$4.33e+10$	-0.25	$2.74e+06$
25	$HO_2 + NH_2 \rightleftharpoons NH_3 + O_2$	$4.46e+15$	-1.87	$1.30e+06$	$2.07e+15$	-1.90	$1.28e+06$
26	$HO_2 + NH_2 \rightleftharpoons NH_3 + O_2$	$5.32e+04$	1.60	$-5.44e+06$	$4.37e+04$	1.61	$-5.43e+06$
27	$HO_2 + NH_2 \rightleftharpoons H_2O + HNO$	$2.13e+06$	0.78	$-5.65e+06$	$2.74e+06$	0.77	$-5.69e+06$
28	$NH_2 + NO \rightleftharpoons NNH + OH$	$4.35e+07$	0.29	$-3.52e+06$	$2.98e+07$	0.29	$-3.53e+06$
29	$NH_2 + NO \rightleftharpoons H_2O + N_2$	$2.80e+16$	-2.35	$3.61e+06$	$1.29e+16$	-2.36	$3.62e+06$
30	$NH_2 + NO_2 \rightleftharpoons H_2O + N_2O$	$3.17e+15$	-2.16	$1.91e+06$	$2.64e+15$	-2.21	$1.95e+06$
31	$NH + NH_2 \rightleftharpoons H + N_2H_2$	$1.32e+12$	-0.47	$0.00e+00$	$2.19e+12$	-0.47	$0.00e+00$
32	$H + NH \rightleftharpoons H_2 + N$	$1.58e+08$	0.71	$3.87e+06$	$3.87e+08$	0.70	$3.92e+06$
33	$NH + OH \rightleftharpoons H_2O + N$	$6.87e+03$	1.73	$-2.29e+06$	$7.55e+03$	1.74	$-2.29e+06$
34	$NH + NH_2 \rightleftharpoons N + NH_3$	$9.39e+00$	2.48	$4.52e+05$	$9.97e+00$	2.50	$4.39e+05$
35	$NH + O \rightleftharpoons H + NO$	$3.46e+10$	0.02	$3.93e+05$	$8.77e+10$	0.02	$3.89e+05$
36	$NH + OH \rightleftharpoons H + HNO$	$2.71e+11$	-0.34	$-1.86e+05$	$2.80e+11$	-0.35	$-1.88e+05$
37	$NH + O_2 \rightleftharpoons HNO + O$	$2.31e+06$	1.03	$4.77e+07$	$1.43e+06$	1.03	$4.90e+07$
38	$NH + O_2 \rightleftharpoons NO + OH$	$4.28e+05$	0.79	$5.04e+06$	$3.95e+05$	0.79	$5.01e+06$
39	$2\,NH \longrightarrow H_2 + N_2$	$9.59e+09$	-0.03	$-6.23e+05$	$1.93e+10$	-0.03	$-6.36e+05$
40	$2\,NH \longrightarrow 2\,H + N_2$	$9.06e+10$	-0.03	$-6.23e+05$	$2.00e+10$	-0.03	$-6.28e+05$
41	$N + NH \rightleftharpoons H + N_2$	$4.97e+08$	0.51	$7.95e+04$	$4.48e+08$	0.51	$7.95e+04$
42	$NH + NO \rightleftharpoons H + N_2O$	$2.24e+11$	-0.52	$-2.85e+06$	$2.20e+11$	-0.50	$-2.85e+06$
43	$NH + NO \rightleftharpoons N_2 + OH$	$4.89e+11$	-0.76	$8.37e+04$	$8.54e+11$	-0.72	$8.37e+04$
44	$NH + NO_2 \rightleftharpoons HNO + NO$	$6.14e+09$	0.00	$0.00e+00$	$9.88e+09$	0.00	$0.00e+00$
45	$N + OH \rightleftharpoons H + NO$	$3.65e+10$	0.00	$0.00e+00$	$1.77e+10$	0.00	$0.00e+00$
46	$N + O_2 \rightleftharpoons NO + O$	$1.09e+07$	1.00	$2.68e+07$	$1.97e+07$	1.01	$2.68e+07$
47	$N + NO \rightleftharpoons N_2 + O$	$1.22e+07$	0.93	$-5.36e+06$	$1.03e+07$	0.91	$-5.42e+06$
48	$N_2H_2 + M \rightleftharpoons H + NNH + M$	$3.38e+40$	-7.58	$3.10e+08$	$4.99e+40$	-7.62	$3.04e+08$
49	$H + N_2H_2 \rightleftharpoons H_2 + NNH$	$5.04e+05$	1.78	$3.08e+06$	$4.20e+05$	1.81	$3.08e+06$
50	$N_2H_2 + OH \rightleftharpoons H_2O + NNH$	$6.70e+00$	2.81	$-2.00e+06$	$6.91e+00$	2.85	$-2.01e+06$
51	$N_2H_2 + NH_2 \rightleftharpoons NH_3 + NNH$	$2.48e+02$	2.25	$-4.08e+06$	$3.32e+02$	2.26	$-4.09e+06$
52	$N_2H_2 + NO \rightleftharpoons N_2O + NH_2$	$4.74e+09$	0.00	$4.95e+07$	$2.46e+09$	0.00	$5.00e+07$
53	$NNH \rightleftharpoons H + N_2$	$2.87e+08$	0.00	$0.00e+00$	$3.99e+08$	0.00	$0.00e+00$
54	$NNH + O_2 \rightleftharpoons HO_2 + N_2$	$7.11e+11$	-0.34	$-5.10e+04$	$2.91e+11$	-0.37	$-5.44e+04$
55	$NNH + OH \rightleftharpoons H_2O + N_2$	$3.59e+10$	0.00	$0.00e+00$	$2.91e+10$	0.00	$0.00e+00$
56	$NNH + NO \rightleftharpoons HNO + N_2$	$3.63e+10$	0.00	$0.00e+00$	$1.51e+11$	0.00	$0.00e+00$
57	$NNH + O \rightleftharpoons NH + NO$	$3.63e+08$	0.38	$-1.62e+06$	$2.22e+08$	0.37	$-1.63e+06$
58	$NNH + O \rightleftharpoons H + N_2O$	$1.50e+11$	-0.23	$-8.87e+04$	$5.05e+10$	-0.24	$-9.20e+04$
59	$HO_2 + NO \rightleftharpoons NO_2 + OH$	$2.36e+09$	0.00	$-1.97e+06$	$1.49e+09$	0.00	$-1.97e+06$
60	$NO + O (^+M) \rightleftharpoons NO_2 (^+M)$	$1.10e+12$	-0.73	$0.00e+00$	$1.53e+12$	-0.68	$0.00e+00$
61	$H + NO_2 \rightleftharpoons NO + OH$	$2.92e+08$	0.85	$-4.44e+06$	$2.45e+08$	0.83	$-4.39e+06$
62	$NO_2 + O \rightleftharpoons NO + O_2$	$4.72e+12$	-0.99	$2.26e+05$	$1.42e+12$	-0.94	$2.30e+05$
63	$NO_2 + O \rightleftharpoons NO + O_2$	$7.33e+13$	-0.82	$5.11e+07$	$9.14e+12$	-0.83	$5.20e+07$
64	$N_2O (^+M) \rightleftharpoons N_2 + O (^+M)$	$1.09e+11$	0.00	$2.41e+08$	$1.77e+11$	0.00	$2.40e+08$
65	$H + N_2O \rightleftharpoons N_2 + OH$	$7.55e+04$	1.82	$5.58e+07$	$6.12e+04$	1.82	$5.54e+07$
66	$N_2O + O \rightleftharpoons 2\,NO$	$9.81e+12$	-0.54	$1.17e+08$	$6.06e+12$	-0.50	$1.15e+08$
67	$N_2O + O \rightleftharpoons N_2 + O_2$	$4.06e+09$	0.00	$6.73e+07$	$8.99e+09$	0.00	$6.56e+07$
68	$N_2O + OH \rightleftharpoons HO_2 + N_2$	$1.30e-05$	4.75	$1.53e+08$	$1.30e-05$	4.73	$1.50e+08$
69	$N_2O + NO \rightleftharpoons N_2 + NO_2$	$5.20e+02$	2.26	$1.91e+08$	$5.94e+02$	2.30	$1.95e+08$
70	$H + HNO \rightleftharpoons H_2 + NO$	$8.04e+07$	0.94	$2.06e+06$	$9.43e+07$	0.92	$2.03e+06$
71	$NH_3 + NO \rightleftharpoons HNO + NH_2$	$1.45e+00$	3.15	$2.27e+08$	$1.45e+00$	3.09	$2.30e+08$
72	$HNO + O \rightleftharpoons NO + OH$	$1.98e+10$	0.00	$0.00e+00$	$5.35e+09$	0.00	$0.00e+00$
73	$HNO + OH \rightleftharpoons H_2O + NO$	$1.07e+06$	1.18	$1.39e+06$	$8.98e+05$	1.15	$1.41e+06$
74	$HNO + O_2 \rightleftharpoons HO_2 + NO$	$1.39e+10$	0.00	$5.91e+07$	$9.62e+09$	0.00	$5.92e+07$
75	$H_2 + N_2O \rightleftharpoons H_2O + N_2$	$6.27e+09$	0.00	$1.36e+08$	$9.16e+09$	0.00	$1.38e+08$

References

[1] Y. Zhang, O. Mathieu, E. L. Petersen, G. Bourque, and H. J. Curran, "Assessing the predictions of a NOx kinetic mechanism on recent hydrogen and syngas experimental data," *Combustion and Flame*, vol. 182, pp. 122–141, 2017.

[2] http://c3.nuigalway.ie/combustionchemistrycentre.

[3] N. Jaouen, L. Vervisch, P. Domingo, and G. Ribert, "Automatic reduction and optimisation of chemistry for turbulent combustion modelling: Impact of the canonical problem," *Combust. Flame*, vol. 175, pp. 60–79, 2017.

[4] N. Jaouen, H. Nguyen, P. Domingo, and L. Vervisch, "Orch: A package to reduce and optimize chemical kinetics. application to tetrafluoromethane oxidation," *SoftwareX*, vol. 27, p. 101819, 2024.

[5] C. K. L. T. Lu, "A directed relation graph method for mechanism reduction," *Proceedings of the Combustion Institute*, vol. 30, pp. 1333–1341, January 2005.

[6] P. Pepiot-Desjardins and H. Pitsch, "An efficient error-propagation-based reduction method for large chemical kinetic mechanisms," *Combustion and Flame*, vol. 154, pp. 67–81, 2008.

[7] J. McCall, "Genetic algorithms for modelling and optimisation," *Journal of Computational and Applied Mathematics*, vol. 184, pp. 205–222, 2005.

[8] Https://github.com/Cantera/cantera/releases/tag/v2.6.0b2.

[9] R. W. Bilger, S. H. Starner, and R. J. Kee, "On reduced mechanisms for methane/air combustion in nonpremixed flames," *Combust. Flame*, vol. 80, no. 2, pp. 135–149, 1990.

[10] A. Masri and R. Barlow, "On conserved scalars that preserve stoichiometric mixture fraction," *Combustion and Flame*, vol. 260, p. 113224, 2024.

[11] A. Liñán, P. Orlandi, R. Verzicco, and F. J. Higuera, "Effects of non-unity lewis numbers in diffusion flames," in *Studying turbulence using numerical databases - V*. CTR, Stanford U., 1994, pp. 5–18.